Available online at www.sciencedirect.com
SCIENCE DIRECT
Tectonophysics 417 (2006) 285–304
TECTONOPHYSICS
www.elsevier.com/locate/tecto

Trenching studies of active faults in Kamchatka, eastern Russia: Palaeoseismic, tectonic and hazard implications

A. Kozhurin [a,*], V. Acocella [b], P.R. Kyle [c], F.M. Lagmay [d], I.V. Melekestsev [e], V. Ponomareva [e], D. Rust [f], A. Tibaldi [g], A. Tunesi [g], C. Corazzato [g], A. Rovida [g], A. Sakharov [h], A. Tengonciang [d], H. Uy [d]

[a] *Geological Institute, Pyzhevsky per. 7, Moscow, 119017, Russia*
[b] *Dipartimento Scienze Geologiche, University of Roma Tre, Roma, Italy*
[c] *Department of Earth and Environmental Science, New Mexico Institute of Mining and Technology, Socorro, NM 87801-4796, USA*
[d] *National Institute of Geological Sciences, Quezon City, Philippines*
[e] *Institute of Volcanology and Seismology, Piip Blvd, 9, Petropavlovsk-Kamchatsky, 683006, Russia*
[f] *Department of Geography and Earth Sciences, Brunel University, Uxbridge, United Kingdom*
[g] *Department of Geological Sciences and Geotechnologies, University of Milan-Bicocca, Milan, Italy*
[h] *Faculty of Soil Science, Moscow State University, Vorobjevy Gory, Moscow 119899, Russia*

Received 14 January 2005; received in revised form 1 January 2006; accepted 28 January 2006
Available online 20 March 2006

Abstract

The central part of the Kamchatka Peninsula is characterized by a well defined depression associated with active volcanism, aligned NE–SW. On the east, the depression is bounded by a prominent system of active faults known as the East Kamchatka Fault Zone (EKFZ). In order to improve understanding of the behaviour and kinematic role of this fault zone a fieldwork programme, including study of trenches, was conducted in the north-central part of this system. Aerial photograph analysis, ground-truthed, indicates a westward fault dip with predominantly normal slip, while lateral offsets of river terraces and stream channels demonstrate a combined dextral component. Over 20 excavated pits and natural exposures were examined to confirm a detailed tephra succession extending from the early Holocene to recent historic eruptions. This chronological framework then provided age control on five past faulting events recognised in three trenches. These events took place at about 10.5, 6.0, 4.5 and, in a two-event succession within a short time span, at 3.3–3.2 ka BP. Event clustering may be characteristic and fault length–displacement values suggest earthquakes of M6.5, thus representing a significant new element in regional seismic hazard evaluations; additional to events generated at the subduction interface. The relatively long gap in faulting since the two most recent events may also be significant for hazard scenarios and there is a possible link between the faulting and volcanic activity in the depression. Overall, the EKFZ, together with the Nachiki Transverse Zone farther south, is thought to define a regional-scale block that is extending eastwards independently from the rest of Kamchatka.

Keywords: Kamchatka; Active faults; Trenching; Palaeoseismology; Tephra; Soil–pyroclastic sequence

* Corresponding author. Fax: +7 095 953 0760.
E-mail addresses: kozhurin@ginras.ru (A. Kozhurin), acocella@uniroma3.it (V. Acocella), kyle@nmt.edu (P.R. Kyle), mlagmay@nigs.upd.edu.ph (F.M. Lagmay), ponomareva@ginras.ru (V. Ponomareva), derek.rust@brunel.ac.uk (D. Rust), alessandro.tibaldi@unimib.it (A. Tibaldi), alx-sakh@yandex.ru (A. Sakharov).

0040-1951/$ - see front matter © 2006 Elsevier B.V. All rights reserved.
doi:10.1016/j.tecto.2006.01.004

1. Introduction

Studies aimed at identifying, mapping and characterising active faults above subduction zones, especially in Holocene volcanic arcs, are crucial in understanding the tectonics and geodynamics of such plate boundaries. In particular, their applicability includes: 1) estimates of tectonic deformation rates; 2) seismic hazard evaluation; 3) relationship with volcanic activity in the arc. The latter application may involve several aspects. At depth, far-field tectonic stresses can cause coseismic crustal failure that, in turn, controls the movement of magma. At the surface, faulting deforms volcanic edifices, possibly inducing sector collapse or influencing the evolution of structures associated with calderas and resurgence during episodes of unrest, as well as controlling the alignment of vents. Moreover, Holocene arc settings offer the relatively unexplored possibility of carrying out palaeoseismic investigations using trench excavations in volcanic deposits. This methodology can provide insights into temporal relationships between tectonics and volcanism using a multidisciplinary approach involving palaeoseismology, structural geology, volcanology and tephrochronology.

The subducting and overriding plates of the Kamchatka volcanic arc are likely to have a strong coupling, as suggested by the frequent high-magnitude earthquakes of the region (Gorbatov et al., 1997), but at the same time volcanism is widespread and displays a high magma output rate (Fedotov and Masurenkov, 1991). Furthermore, recent reverse faults have been inferred close to the most magma-productive areas of the arc (Geist and Scholl, 1994). However, despite these intriguing aspects, most of the previous work carried out on recent tectonics in Kamchatka has concentrated on various aspects of the subduction process and not included field-based structural neotectonic data (Kepezhinskas, 1987; Hochstaedter et al., 1994; Fedorov and Shapiro, 1998; Levin et al., 2002).

In the present paper we describe field evidence of Holocene faulting in northern Kamchatka and the results of the first palaeoseismic trenching study across an active fault carried out in the Kamchatka Peninsula. In particular, we use structural evidence of past earthquakes, combined with known volcanic eruption markers, to reconstruct a palaeoseismic history. Our methodology combines field and aerial photograph examination of fault structures and offset features, detailed studies of tephra stratigraphy within artificial and natural exposures, ^{14}C dating, and logging of trench wall exposures created in excavations across active fault scarps. The results allow us to define a major active fault system crossing the Kamchatka Peninsula, characterise its kinematics and geometry, and document the occurrence of several major Holocene faulting events. Additionally, the methodology provides an example of palaeoseismic investigations in volcanic terrain as well as assessing the seismic hazards and geodynamic characteristics of this plate boundary.

2. Geological and neotectonic setting

The Kamchatka Peninsula marks the northwestern margin of the Pacific plate and is one of the most tectonically active regions of the world (Gorbatov et al., 1997). It is thought to belong to either the North American plate (DeMets et al., 1990) or to the separate Okhotsk plate (Zonenshain and Savostin, 1979) that may be bounded in the north by either the North American plate or the Bering microplate (Lander et al., 1994; Mackey et al., 1997) (Fig. 1). The study area lies inboard of the northern end of the Kamchatka–Kurile trench, close to the junction with the Aleutian–Komandorsky chain that is believed to be colliding with Kamchatka at the Kamchatsky Peninsula Cape (Geist and Scholl, 1994; Gaedicke et al., 2000; Fig. 1). Slab dip here is believed to reduce from 55° to 35°, with the probable loss of a slab fragment producing a westwards step in the volcanic front with the formation of the volcanoes of the Kliuchevskoi group and the more isolated Shiveluch volcano (Yogodzinski et al., 2001; Levin et al., 2002; Park et al., 2002).

Kamchatka contains about 30 active volcanoes and hundreds of monogenetic vents. Recent volcanism in Kamchatka is highly explosive (Melekestsev, 1980); numerous tephra horizons interlayered with palaeosols mantle the topography. Most of the instrumentally recorded seismicity in Kamchatka is related to the subduction of the Pacific plate at a present rate of 9–10 cm year^{-1} (Geist and Scholl, 1994). Earthquakes within the peninsula crust, above the subduction zone, are rare and of moderate magnitudes (Gordeev et al., 2004), and show no clear correlation with the major fault systems of Kamchatka. The present-day structure and tectonics of Kamchatka is reflected in the topography (Fig. 2) and reveals margin-parallel uplifted and subsided blocks, a regime replacing the thrust dominated pre-Pliocene tectonics related to terrane collision (e.g. Konstantinovskaya, 2003, and references therein).

The first-order elements of the present-day structure of Central Kamchatka are the Central Kamchatka Depression (CKD), with ranges to the west (the Sredinny Range) and east (East Kamchatka Ranges),

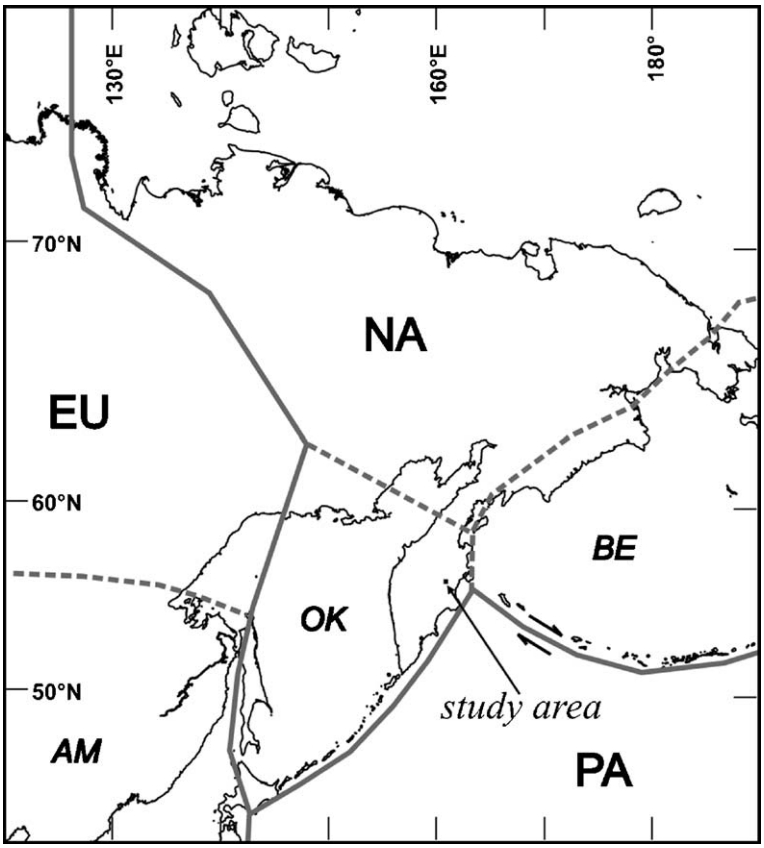

Fig. 1. Plate boundaries configuration in NW Pacific. Dashed lines are boundaries of minor plates within major plates. NA = North American Plate, EU = Eurasian Plate, PA = Pacific Plate (DeMets et al., 1990). AM = Amurian Plate, OK = Okhotsk Plate (Zonenshain and Savostin, 1979), BE = Bering Sea Plate (Lander et al., 1994).

and a separate elevated zone made up of three promontories on the eastern side of the peninsula (Fig. 2). Southern Kamchatka is much less structurally and topographically differentiated and its northern boundary can be drawn along the NW–SE striking lineament known as the Nachiki Transverse Zone (NTZ in Fig. 2) that terminates at the southern end of the CKD.

With its western gently sloping flank and steep faceted eastern flank, the CKD is clearly asymmetric. In plan-view, the depression widens to the north where the Kliuchevskoi group of volcanoes and isolated Shiveluch volcanic massif are located; while the larger southern portion of the CKD remains entirely free of recent volcanism. North of the Shiveluch volcano the depression becomes more symmetric and the thick Quaternary fill and volcanism are absent. Formation of the CKD dates back to at least the Late Pliocene, though its present morphology developed mainly during middle–late Quaternary time (Melekestsev, 1974). Total thickness of the sedimentary fill of the depression exceeds 300 m (Braitseva et al., 1968).

The contrasting structural and topographic development of the central part of the peninsula has been accompanied by volcanism concentrated in three main belts (Fig. 2). First, a volcanic belt extends along the crest of the Sredinny Range, west of the CKD. Second, the Eastern Volcanic Front (EVF) lies between the East Kamchatka Ranges and the distinctive capes on the eastern margin of the peninsula. Volcanic centres of the EVF are generally aligned NNE but not exactly parallel to the CKD eastern boundary. In the southern part of this belt, several volcanoes (Zhupanovskie Vostriaki and, farther south, Avachinsky, Koriaksky and Kozel'sky) are aligned NW–SE, parallel to the Nachiki Transverse Zone. In south Kamchatka volcanism occurs as an extension of the EVF, with a volcanic-free gap coinciding with the NTZ. Finally, the prominent volcanoes of the northern part of the CKD represent the relatively short third volcanic belt (Fig. 2). A connection between these volcanoes and the EVF can be established via the Kizimen volcano, which is located on the slopes of the

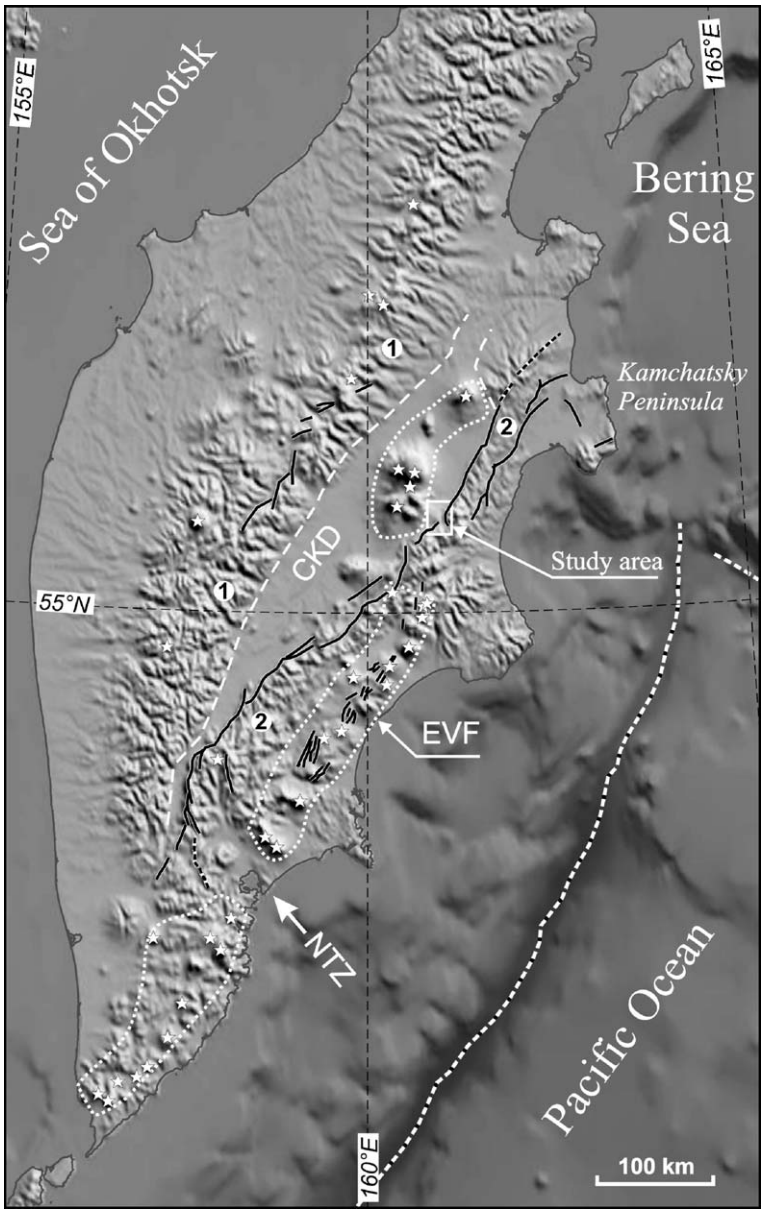

Fig. 2. Major neotectonic elements of the Kamchatka Peninsula. Solid black lines are active faults, dashed lines where inferred. NTZ=Nachiki Transverse Zone, CKD=Central Kamchatka Depression. Numbers in circles: 1—Sredinny Range, 2—East Kamchatka Ranges. White stars mark major Holocene volcanic centres, areas bounded by dotted white lines are volcanic zones; EVF=Eastern Volcanic Front (see text). Dashed lines within the Pacific Ocean are axes of the Kurile–Kamchatka and west Aleutian deep-sea trenches.

mountain ranges making up the eastern flank of the CKD (Fig. 3).

3. Late Quaternary faults of Kamchatka

3.1. East Kamchatka Fault Zone

The evident asymmetry of the CKD suggests the existence of a major fault zone with large-scale vertical displacement on its eastern margin, which hereinafter we will refer to as the East Kamchatka Fault Zone (EKFZ). Using topographic relief alone, the vertical component of differential movement, accumulating on the fault zone over the mid-late Quaternary period, amounts to 1 to 1.5 km. If the thickness of the CKD fill is included, this value may increase to about 2 km.

Svyatlovsky (1967) and Tikhonov (1968) proposed two different interpretations for the vertical movement

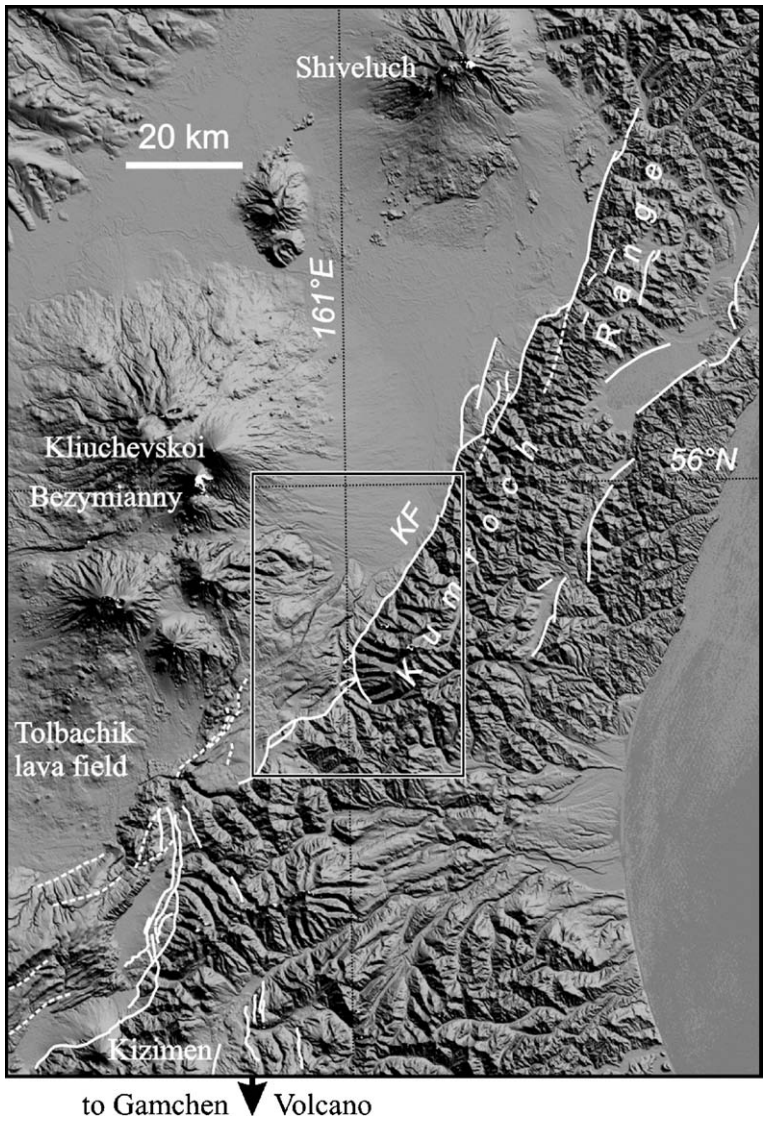

Fig. 3. SRTM shaded relief image of the northern part of the Central Kamchatka Depression. White lines are major active faults, dashed where inferred; KF = the Kumroch Fault (see text). Rectangle marks the area shown in Fig. 4.

on the fault zone: normal and reverse respectively. Erlich (1973) identified the fault, which he referred to as the Kamchatka Frontal Face fault, as having dominantly normal sense vertical movements. All later studies provide additional geomorphic evidence for a normal sense of vertical fault displacement between the elevation of the East Kamchatka Ranges and the CKD (Legler, 1976; Kozhurin, 1988, 1990).

Much more debatable has always been the question whether any horizontal movements were occurring on the fault zone. Based on the en echelon plan-view arrangement of Z-shaped individual ranges within the elevation of the East Kamchatka Ranges and the presence of approximately N–S-striking graben between the ranges, Erlich (1973) inferred a component of along-strike extension, although no strike-slip offsets of geomorphic features along individual faults of the system were observed (Erlikh et al., 1974). Legler (1976) came to the conclusion that movements along the fault zone were dominantly left-lateral. In his model the fault zone is regarded as the western boundary of a block that has been moving northeast throughout the Quaternary due to the oblique Pacific plate/arc interaction. Legler's model also predicts that this left-lateral back-arc strike-slip faulting affects only the northern half of

the Kamchatka–Kurile arc, and that in the southern Kuriles the sense of strike-slip faulting must change to right-lateral.

As shown by detailed interpretation of aerial images (Legler, 1976; Kozhurin, 1988), the EKFZ is a) composed of over a hundred individual faults and, b) extends to the north beyond the limits of the CKD with several NE–SW-striking faults occurring within the eastern slopes of the Kumroch Range (the northernmost of the East Kamchatka Ranges), and within the Kamchatsky Peninsula (Fig. 2). Kozhurin (1988, 1990) examined the geomorphic expression of late Quaternary fault movements, finding that the lateral component is dextral and roughly comparable in magnitude to the dip-slip component.

3.2. Faults in the Sredinny Range

Geometrically similar to the EKFZ, but shorter, is a fault system, striking NNE–SSE, interpreted from remotely sensed images and topography, which cuts the crest of the Sredinny Range west of the CKD (Kozhurin, 2004; Fig. 2). Individual faults show downthrow to the west and their arrangement suggests a right-lateral component of movement.

3.3. Faults of the Eastern Volcanic Front

Another area of active faulting in Kamchatka is the EVF (Fig. 2). These faults exhibit dominantly normal displacement, probably with a small left-

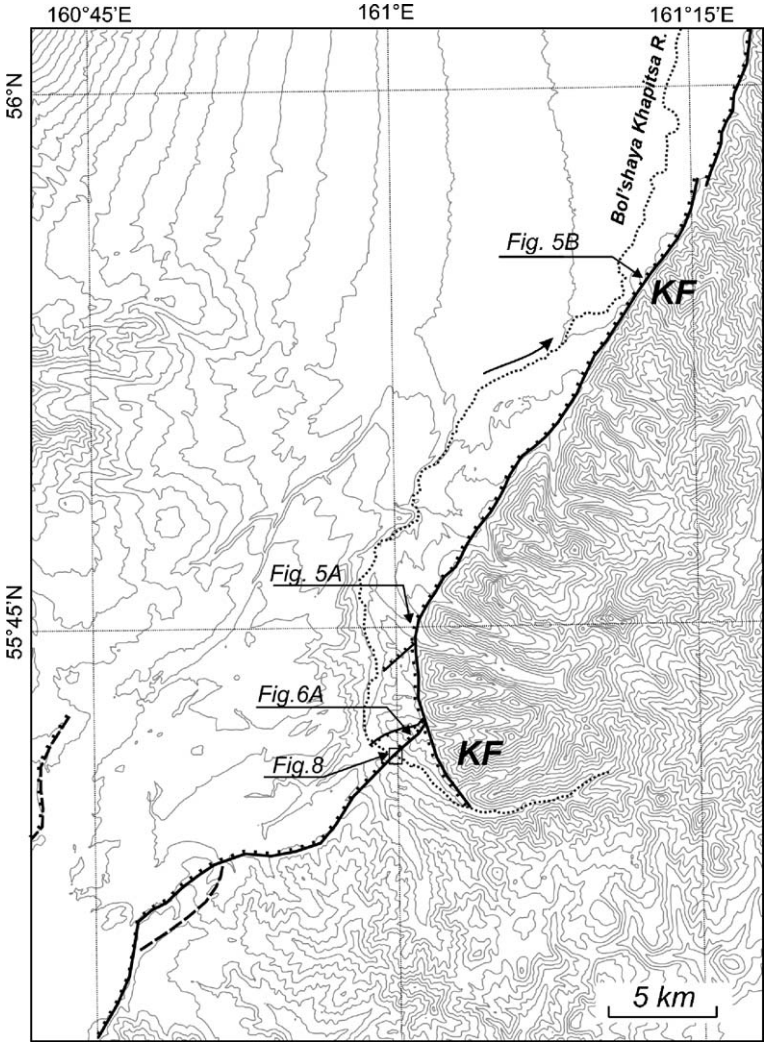

Fig. 4. Active faults of the south Kumroch Range area. Solid black lines are faults, dashed where inferred, ticks on downthrown side. Relief of the area is shown by topographic contour lines with contour interval of 100 m. KF = Kumroch fault.

lateral component, producing a graben-in-graben structure about 130 km long and 10–18 km-wide, along the axis of the belt (Florensky and Trifonov, 1985). Characteristics of the fault zone are, 1) northward narrowing of the fault belt and its termination where the volcanic belt ends and, 2) segmentation with steps coinciding with large calderas.

4. Study area: the Kumroch Range segment of the East Kamchatka Fault Zone

We studied the CKD boundary faults in the southern Kumroch Range area with the aim of determining their geomorphic expression, together with their late Quaternary kinematics and palaeoseismology. In this area, the EKFZ is represented by several fault traces. In the north this fault is called, after Legler (1976), the Kumroch fault (Figs. 3 and 4). Using photogrammetry, Demina V. V. (in Svyatlovsky, 1967) determined a dip angle of 65–70° west for the fault. Together with the east-side-up geometry this indicates normal-sense vertical movement along the fault.

The Kumroch fault offsets moraines of the last (Q^4_{III}) glaciation, post-glacial terraces and debris fans (Fig. 5A). Maximum postglacial vertical offset of late Pleistocene moraine surfaces is 27–30 m. Since the age of the moraine surface is estimated to be between 11500 and 14000 calibrated years BP (Melekestsev, personal communication), the rate of vertical movement is approximately 2.0–2.5 mm year^{-1}. There is also evidence for a component of right-lateral movement on the fault (Kozhurin, 1990; Fig. 5B), comparable to that of the normal component.

At the southern end of the Kumroch Range the Kumroch fault bends to a NE–SW strike and branches into three splay faults (see Fig. 4). Two of these faults are relatively short, while the third (southeastern) fault extends farther south. It crosses the Bol'shaya Khapitsa valley producing a prominent scarp, though significantly lower that that of the Kumroch fault (about 200 m and

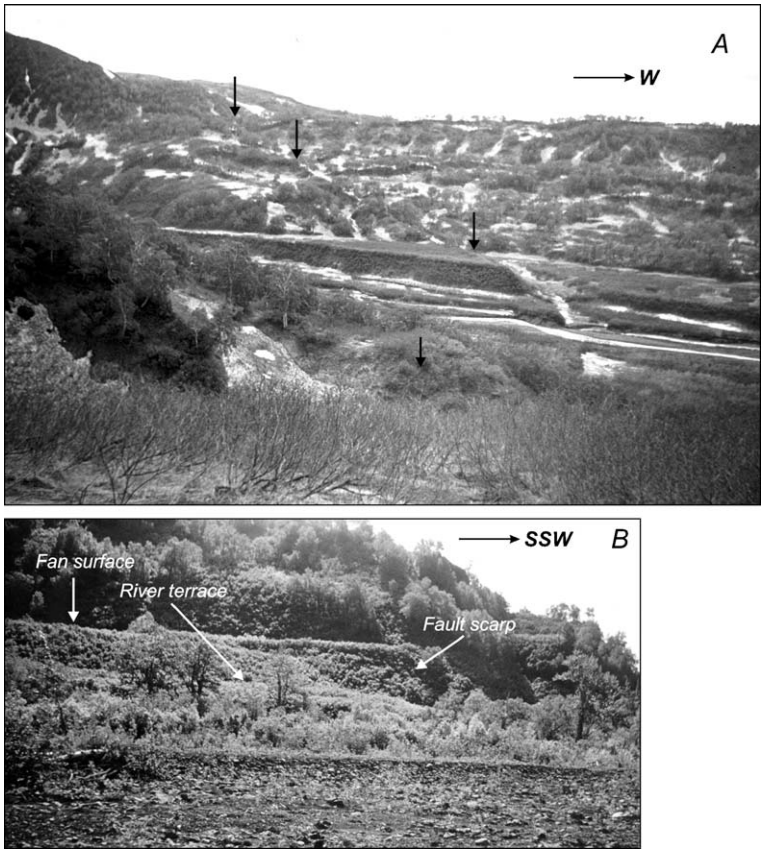

Fig. 5. (A) Fault scarp (marked by black arrows) of the main trace of the Kumroch fault, bordering the southern Kumroch Range, where it cuts postglacial terraces of one of the tributaries to the B.Khapitsa River. Note that on climbing the valley side the fault turns east, indicating westward dip of the fault plane. Viewed to south. (B) Approximately 15 m right-lateral offset of a river terrace formed at a large Late Pleistocene fan, Central Kumroch Range, Topolovaya River, view WSW.

1000 m high, respectively). Thus, south of the Kumroch Range, this fault forms the principal boundary between the CKD and East Kamchatka Ranges. Several observations in and north of the Bol'shaya Khapitsa valley suggest that the fault, in the same way as the Kumroch fault, combines roughly equal right-lateral and vertical movements (Fig. 6).

For our trenching investigation we chose this southeastern fault because, firstly, it provides continuity of the EKFZ and is therefore likely to be representative of the EKFZ and accommodate a significant proportion of its displacement. Secondly, it cuts well-developed river terraces that provide favourable conditions for trenching. Finally, the Bol'shaya Khapitsa terraces represent a rare instance where thick vegetation cover is absent and manual digging is easy.

Within the river valley faulting produces north-west-facing scarps across a series of terraces (Figs. 7 and 8, see also Fig. 6B). On the highest river terrace (*t5*), a single scarp is produced with 3.3 m of ground surface vertical separation (profile A in Fig. 8; see also Fig. 11A). On the succeeding terrace (*t4*) the scarp bifurcates into two lower scarps, total amount of vertical separation (across two faults) remaining roughly the same at 3.2 m (profile B in Fig. 8). As the slope angle of the terrace surface between two scarps differs from that east and west of them, only limits on the amounts of vertical separation across

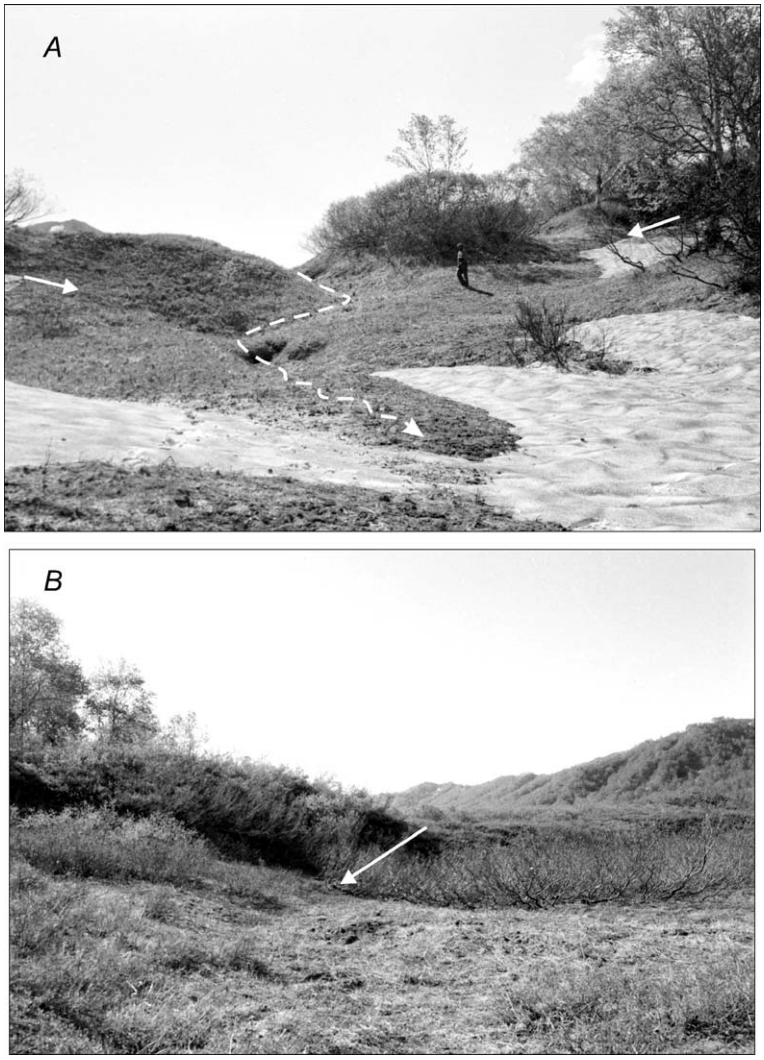

Fig. 6. (A) Combined normal and right-lateral offsets of a shallow gulley (note person for scale). White arrows indicate the base of the fault scarp. White dashed line marks the axis of the displaced gully. View to SSE. (B) Bol'shaya Khapitsa River terrace cut by a NE-striking fault in the southern Kumroch area. White arrow shows base of 3 m high fault scarp. View towards SE.

Fig. 7. Fault scarp on the Bol'shaya Khapitsa River terrace across which the trenches were dug. View to the south. The heavily forested slope in the background is on the southern side of the river.

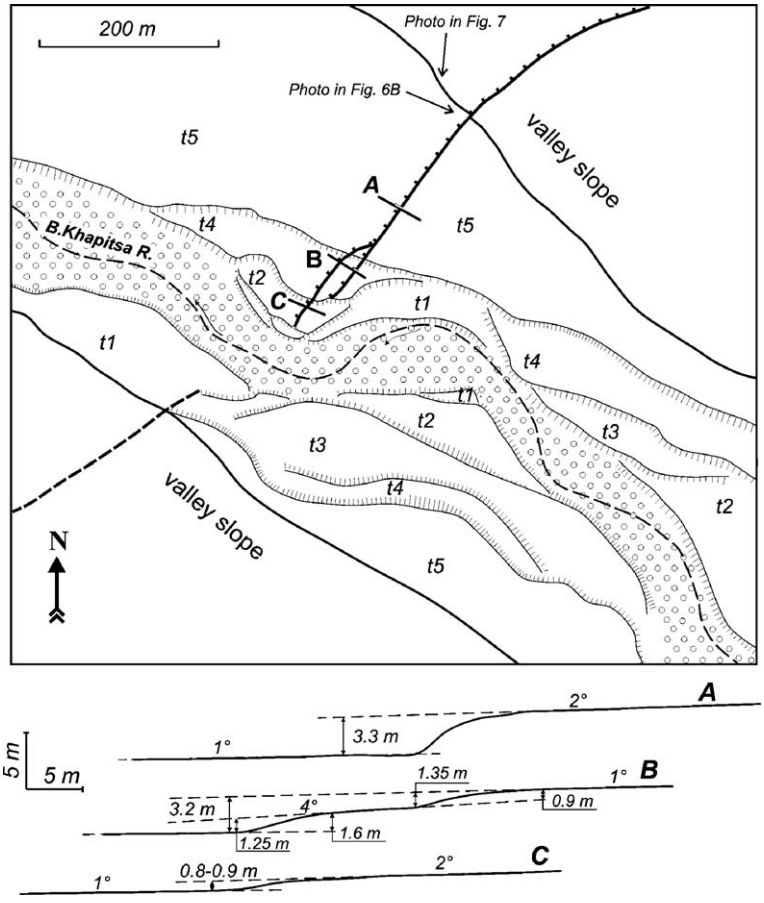

Fig. 8. (Top) Location of topographic profiles and trenches in the Bol'shaya Khapitsa River Valley (lines A, B and C). Thin lines with ticks are terrace risers, terraces marked by *t1* to *t5* from lower to higher, circle-filled is flood terrace. Heavy solid lines are faults, dashed where location is uncertain, ticks on downthrown side. (Bottom) Topographic profiles along lines A, B and C. Original dip of terraces (approximated with dashed lines) and amounts of vertical separation of the terrace surfaces are indicated. For location see Fig. 4.

each scarp separately can be placed (0.9 m–1.35 m and 1.25 m and 1.6 m on profile B in Fig. 8) (Caskey, 1995). On the youngest of the faulted terraces (*t2*), there is again a single scarp with only 0.8–0.9 m of vertical separation (profile C in Fig. 8). The observed decrease in amplitude of vertical ground surface offsets from *t5* to *t2* indicates that the larger surface offset measured is a cumulative vertical displacement. It is likely also that the 0.8–0.9 m vertical offset is a one-event offset and that the terrace *t2* has been ruptured only once. Yet based on the above values it can not be said with certainty by what increments the higher fault scarps have been growing.

Three trenches were dug across the fault scarps, complemented by 22 exploratory pits and natural outcrops excavated within the terrace sequence adjacent to the trenches and more widely in the valley. All these exposures confirmed that the terraces were mantled with a clearly defined succession of pyroclastic deposits with intervening soil development.

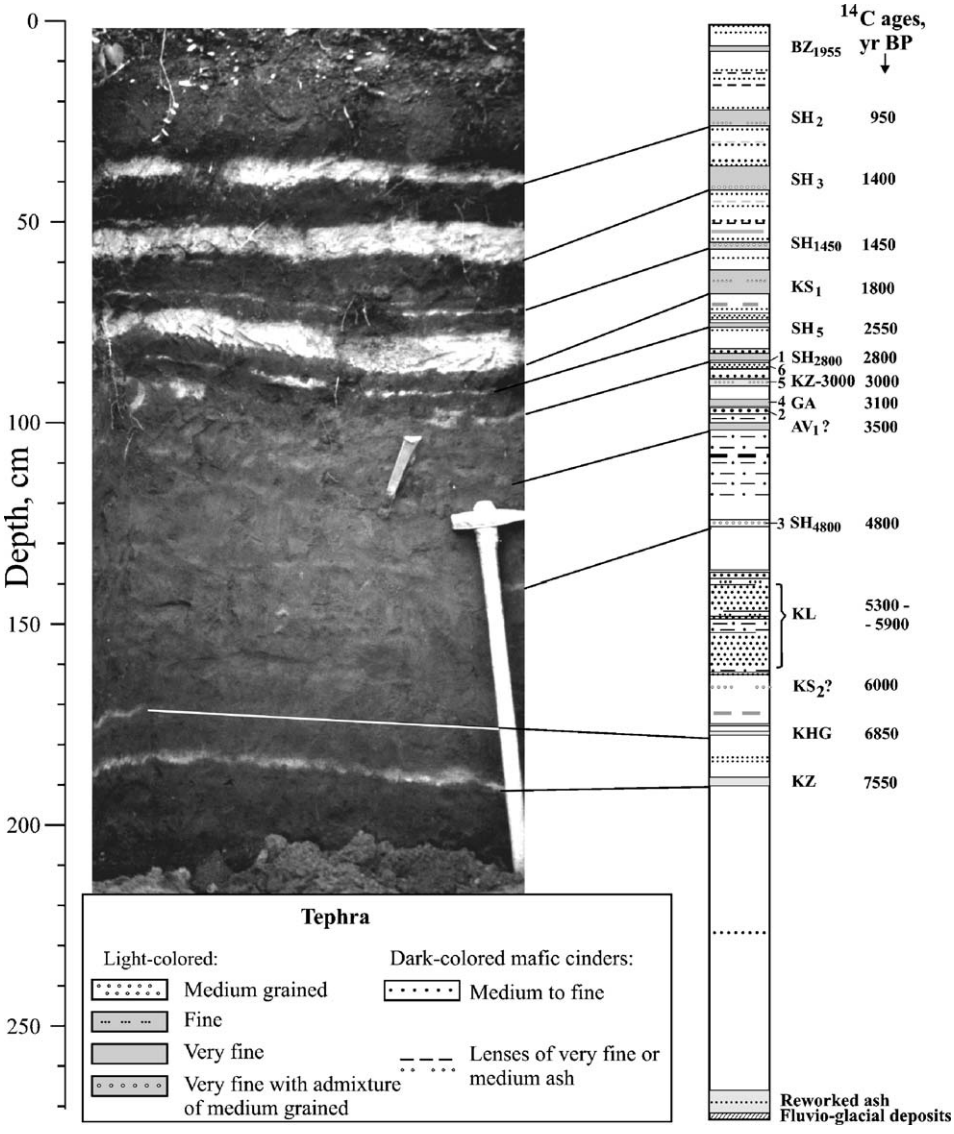

Fig. 9. Summary section of soil–pyroclastic sequence is based on 22 individual excavations and outcrops. Marker tephra layers (from top to bottom): BZ=Bezymianny volcano, SH=Shiveluch, KS=Ksudach, KZ=Kizimen, GA=Gamchen, AV=Avachinsky, KL=Kliuchevskoi, KHG=Khangar. Codes and ^{14}C ages of individual tephra horizons according to Braitseva et al. (1995), Melekestsev et al. (1995), Braitseva et al. (1997a,b, 1998), Pevzner et al. (1998), Bazanova and Pevzner (2001). Radiocarbon ages are rounded to the nearest 50 years. Tephra interspersed with background formation of brown sandy loams and soils. Digits right of the section show tephra samples location.

5. Tephra

The Holocene soil–pyroclastic cover is up to 2.5 m thick and contains tephra layers from most of the adjacent volcanoes (Fig. 9, Table 1). In all, we recognise about 10 tephras, which form continuous layers 1 to 7 cm thick, mostly light-coloured. Tephra layers are separated by palaeosols containing pyroclastic material including dark-coloured cinders and thin lenses of both light and dark ashes. Identifying the tephra layers was based on previous studies that employed extensive radiocarbon dating to reconstruct Holocene eruptive histories for most of the volcanoes and to date their largest explosive eruptions (Braitseva et al., 1984, 1991, 1993, 1995; Melekestsev et al., 1995; Ponomareva et al., 1998, 2002). Holocene marker tephra layers have been studied and dated in many localities in the area of our field site (Braitseva et al., 1984, 1991, 1997b; Pevzner et al., 1998; Ponomareva et al., 1998) and to validate our correlations we sampled a number of tephra layers for subsequent mineralogical and geochemical analyses (Table 2, Fig. 10).

We consider that six marker tephra layers originated from Shiveluch volcano (layers labelled "SH" in Fig. 8), located ~110 km NNE from the study site (see Fig. 3 for location). These are typically pale to yellow-coloured fine to coarse ashes; the distinctive "salt-and-pepper" appearance being due to enrichment by mineral grains in

Table 1
Holocene marker tephra layers in the Bol'shaya Khapitsa River Valley, Kumroch Range, Kamchatka Peninsula

Code	Source volcano	^{14}C ages (years BP)	Cal. ages years BP	Description	Thickness (cm)	Characteristic features
BZ_{1955}	Bezymianny	–	1955 AD	Gray, greenish-grey very fine ash	1–3	Medium K_2O content, presence of Hb
SH_2	Shiveluch	950	900	Fine to very fine pale ash, with lenses of fine "salt-and-pepper" mineral-rich sand at the bottom	3–6	Medium K_2O content, high Cr and Sr content, presence of Hb
SH_3	Shiveluch	1400	1300	Fine to very fine pale ash, lower 1 cm-fine to medium "salt-and-pepper" mineral-rich sand	4–7	Medium K_2O content, high Cr and Sr content, presence of Hb
SH_{1450}	Shiveluch	1450	1350	Dirty-pale ash: coarse "salt-and-pepper" sand at the top and fine ash at the bottom	1–2	Medium K_2O content, high Cr and Sr content, presence of Hb
KS_1	Ksudach	1800	1700	Fine to very fine yellowish-pale ash, with lenses of fine sand in the middle of the layer	4–8	Low K_2O content, absence of Hb
SH_5	Shiveluch	2550	2750	Fine to very fine pale ash	1–2	Medium K_2O content, high Cr and Sr content, presence of Hb
SH_{2800}	Shiveluch	2800	2850	Fine to very fine yellowish-pale ash	2–3	Medium K_2O content, high Cr and Sr content, presence of Hb
KZ-3000	Kizimen	3000	3200	Dirty-beige fine to very fine ash. In places the layer merges into sandy loams due to its colour.	2–3	Medium K_2O content, presence of both mafic and silicic glass, presence of Hb
GA	Gamchen	3100	3300	Dirty-pink fine to very fine ash	0.5–2	Low K_2O content In places these two layers
	Kliuchevskoi?	?		Dark-grey medium to coarse volcanic sand	2	Medium K_2O content merge into one horizon
AV_1 ?	Avachinsky	3500	3800	Bluish-grey very fine to fine ash, tends to merge into sandy loam	1	Basaltic andesitic composition, low K_2O content
SH_{4800}	Shiveluch	4800	5500	Dark-yellow medium "salt-and-pepper" volcanic sand	2	Medium K_2O content, high Cr and Sr content, presence of Hb
KL	Kliuchevskoi	5300–5900	6100–6750	Stratified dark-grey fine to medium volcanic sands with iron-stained layers and thin palaeosols	10–22	Basaltic andesitic composition, medium K_2O content
KS_2 ?	Ksudach	6000	6800	Rare lenses of pumiceous grains	0.5–1	Variable glass composition, absence of Hb, low K_2O content
KHG	Khangar	6850	7650	Fine to very fine light-yellow ash	1–1.5	Medium to high K_2O content, presence of Bi
KZ	Kizimen	7550	8350	Fine to very fine light-yellow ash	2–3	Medium K_2O content, presence of Hb

The tephra layers are listed in chronological order. In column 3, the ages are average radiocarbon ages of the marker tephra layers rounded to the nearest 50 years (Melekestsev et al., 1995; Braitseva et al., 1997a,b; Pevzner et al., 1998; Bazanova and Pevzner, 2001). Age of KL package is estimated based on the dates for initial (Braitseva et al., 1995) and terminal (Bourgeois et al., 2006) eruptions. In column 4, the ^{14}C ages are calibrated to calendar years according to technique by Stuiver et al. (1998) and rounded to nearest 50 years. Hb, hornblende; Ol, olivine; Bi, biotite.

Table 2
Major and selected trace element composition of some marker tephras in the Bol'shaya Khapitsa River Valley

Tephra layers	SH_{2800}	Kliuchevskoi	KZ-3000	Gamchen	Kliuchevskoi	SH_{4800}
Sample numbers	2003-7/1	2003-7/6	2003-7/5	2003-7/4	2003-7/2	2003-7/3
SiO_2	59.73	52.28	61.87	56.20	53.27	58.06
TiO_2	0.68	1.21	0.67	0.85	0.97	0.61
Al_2O_3	17.28	19.28	17.47	20.12	19.71	19.29
Fe_2O_3	6.53	9.98	6.24	8.49	8.63	5.86
MnO	0.12	0.17	0.12	0.16	0.14	0.11
MgO	4.04	4.79	2.74	2.72	5.06	3.75
CaO	6.18	8.53	5.81	7.62	8.22	6.82
Na_2O	3.85	3.04	3.41	3.24	3.15	4.60
K_2O	1.42	0.51	1.56	0.43	0.65	0.79
P_2O_5	0.17	0.21	0.12	0.18	0.18	0.09
Total	100.00	100.00	100.00	100.00	100.00	100.00
Cl	660	329	379	410	283	266
S	142	123	208	184	98	129
Ba	446	307	622	230	352	323
Zr	147	112	120	85	106	138
Sr	426	268	270	252	326	636
Zn	64	82	58	69	80	81
Cu	41	62	18	21	18	16
Ni	37	27	17	67	27	31
Cr	127	96	44	27	75	98

Analyses were made in New Mexico Institute of Mining and Technology. Samples are enlisted in stratigraphical order from top to bottom. For tephra codes and samples location see Fig. 9 (the last digit of the sample number is provided right of the section). Total Fe as Fe_2O_3.

the course of aeolian separation (Braitseva et al., 1997b). Two tephra layers, SH_{2800} and SH_{4800}, important for our palaeoseismic study, have been analysed for major and selected trace elements. Both samples yielded high contents of Cr and Mg (Fig. 10, Table 2). As only Shiveluch products have an adakitic geochemical signature, specifically high Cr and Mg contents within an overall andesitic composition (Braitseva et al., 1997a, b), this provides further evidence for a Shiveluch source for the two tephra layers.

We also conclude that another two marker layers came from Kizimen volcano (75 km SSW). The older tephra layer (KZ, Table 1, Fig. 9) is a well known regional marker (Braitseva et al., 1997b). The younger tephra layer, labelled KZ-3000, was attributed to the Kizimen eruption based on geochemical features typical for Kizimen rocks (Fig. 10) and the presence of both mafic and silicic glass (Melekestsev et al., 1995).

One more tephra, dirty-pink in colour and fine to very fine grained, is well expressed in only a few excavations and was assigned to Gamchen volcano (80 km SSW) based on stratigraphy and geochemical features (labelled Gamchen in Figs. 9 and 10) (Churikova et al., 2001; Melekestsev and Ponomareva, personal communication).

Other regional marker tephra layers came from Ksudach (~500 km SSW; Braitseva et al., 1996; Volynets et al., 1999), and Khangar (250 km SW; Braitseva et al., 1997b; Bazanova and Pevzner, 2001) volcanoes (KS and KHG, respectively, in Fig. 9). Each of these tephra layers has a distinct appearance and mineralogical composition (Table 1) that permits fast and reliable identification.

Layers of dark grey fine to medium-grained pyroclastic material are mostly associated with Kliuchevskoi volcano or its flank eruptions (labelled KL in Fig. 9). Some of them merge into packages of strata, indicating periods of continuous explosive activity. The thickest and best expressed package of this kind, fitting into an age interval of 5300–5900 ^{14}C years BP, has been traditionally associated with the initial eruptions of Kliuchevskoi (Braitseva et al., 1995).

Individual layers of soil–pyroclastic sequences are usually horizontal but in some cases display small-scale convolutions. These structures are interpreted to result from creep within the unconsolidated ash on very low gradients; occurrences observed in some pits on completely flat areas may result from seismic shaking and represent specific seismites.

6. Trench stratigraphy

Three trenches of different sizes were dug across fault scarps cutting the terrace sequence, their locations coinciding with profiles A, B and C (Fig. 8). Below, we concentrate our description on A, the largest and most

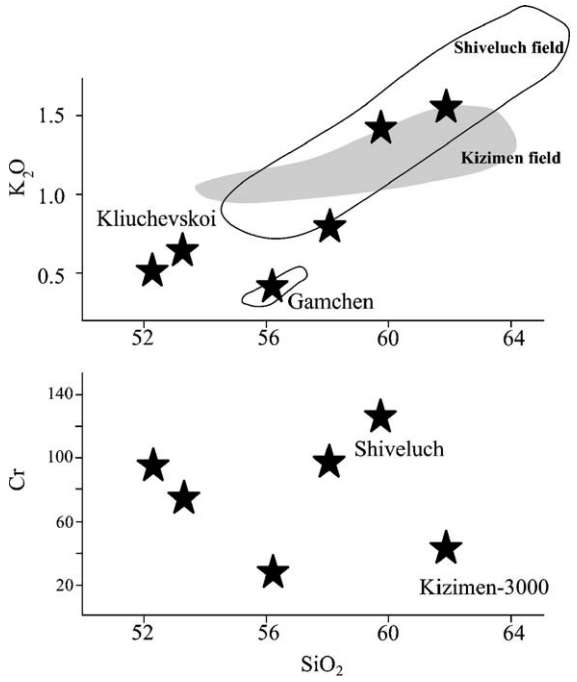

Fig. 10. Geochemical features of selected marker tephras in the Bol'shaya Khapitsa valley. Black stars denote tephra samples collected from the palaeoseismic trenches. Reference data on compositions of Shiveluch tephra are from Braitseva et al. (1997b), Gamchen from Churikova et al. (2001), Kizimen from Melekestsev et al. (1995).

representative in terms of soil–pyroclastic stratigraphy and palaeoseismological features. Information from trench C provided supporting evidence.

The scarp profile on the highest river terrace, where trench A is located, is generally smooth and lacks any indication of multiple fault breaks. In the subsurface the section is composed of two main units: a distinctive soil–pyroclastic sequence in the upper part of the trenches, overlying coarse sub- to well-rounded generally poorly sorted gravels (Fig. 11). The soil–pyroclastic sequence includes two principal constituents. First, there are distinct layers of volcanic tephra and, second, interlayered palaeosols rich in dispersed and altered ash. On the downthrown side of the fault the sequence is a little thicker than on the upthrown side (1.6 m and 1.45 m, respectively). This means that about 15 cm of the cover in the downthrown side accumulated due to scarp slope wash and redeposition of loose material from the upthrown side.

Away from the fault scarp both the ground surface and the buried gravel upper surface show the same original west-directed dip of about 2° (Fig. 11A). Vertical offset amount measured on the gravels (~3.8 m) exceeds that of the land surface (~3.3 m) by only 0.5 m, indicating that scarp growth had limited impact on post-rupture accumulation and distribution of pyroclastic material and in-situ soil development. Below the base of the surface scarp the gravel surface exposures reveal the development of a local graben-like depression filled with mostly slope-derived material. On the outer (western) side of the depression, two small west-dipping faults displace the lowermost horizons of the soil–pyroclastic sequence but do not affect the gravel. Both faults are located above the edges of a graben-like depression and, in our interpretation, probably developed as flexuring-related accommodation structures not directly linked to movements along the major fault plane.

The tephra stratigraphy provides an overall system of isochrons that can be used for fast and reliable estimates for bracketing the age of faulting events. While, in order to estimate a more precise age for an event horizon occurring between the marker tephra layers, we calculate a rate of palaeosol accumulation (0.1–0.4 mm $year^{-1}$) based on known marker tephra layers and palaeosol thicknesses. The uppermost several decimetres of the sequence contain tephra layers continuous throughout the trench exposures, starting with the most recent 1994 ash from Kliuchevskoi volcano and 1955 eruption of Bezymianny (BZ in Fig. 9) down to the SH_{2800} tephra from Shiveluch (see Fig. 11B). These tephra layers are in places distorted, with short segments of the beds sometimes rotated or overlapping, but as a whole these deformation structures can be attributed to gravitational processes on a surface slope alone or to down-slope movement triggered by earthquakes.

Below this upper unfaulted part of the sequence there are several features suggesting incremental fault movements. Most distinct are irregular step-like breaks in the gravel surface and the occurrence of colluvial wedges within the soil–pyroclastic cover. The details are described in the next section.

7. Faulting events

Fig. 11C represents our palaeoseismic interpretation of the section exposed in the southern wall of trench A and should aid understanding of the following enumerated description and analysis.

7.1. Event 1

The two end segments of the buried gravel surface represent the original west dip of about 2° (segments *ab* and *gh* in Fig. 11A). Between, there exist two inclined (segments *bc* and *de*) and two notably steeper segments (segments *cd* and *ef*). We interpret that the segments *bc*

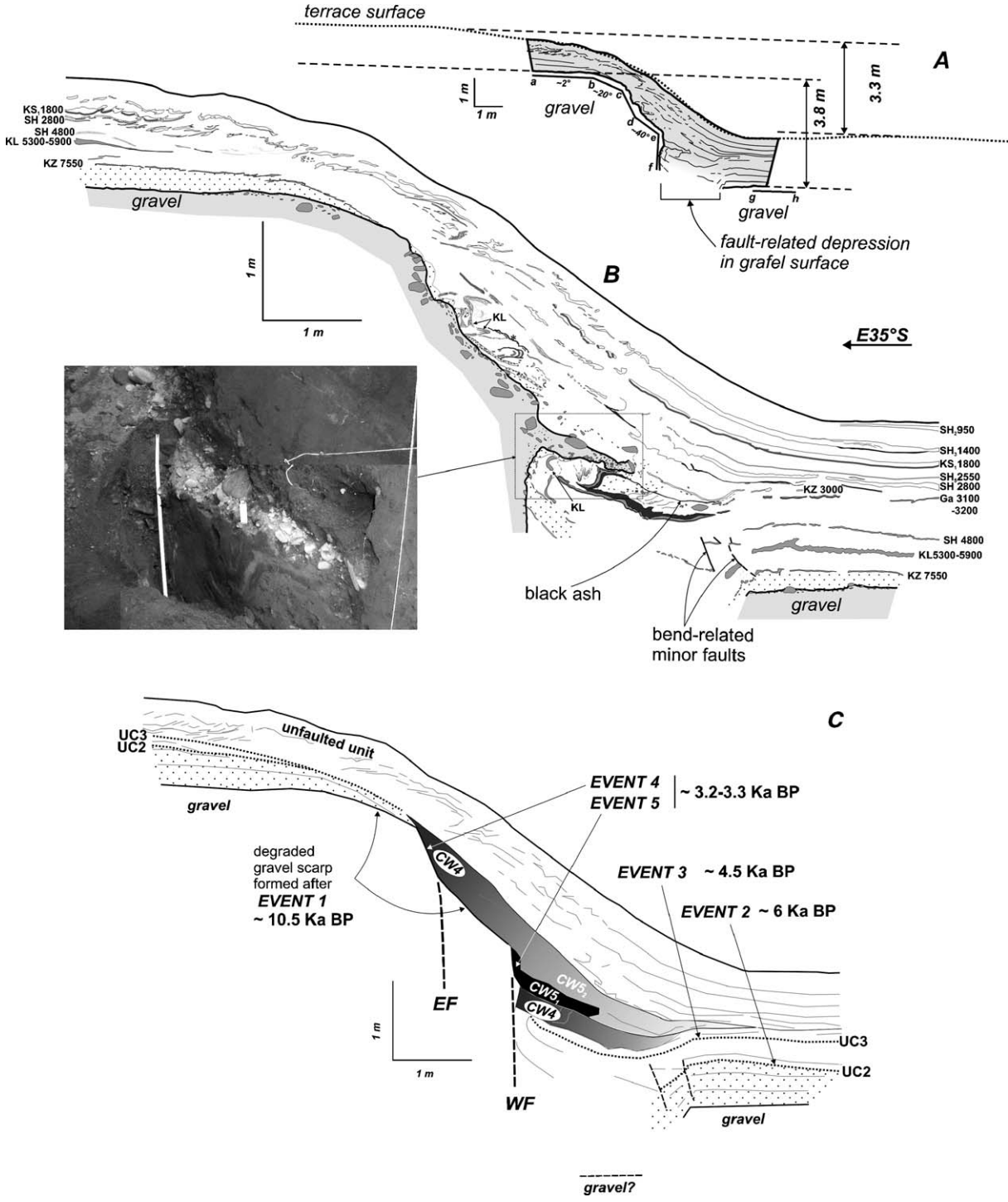

Fig. 11. (A) Measurements of cumulative fault offset: dotted line is profile surface, dashed lines show projections of the original (far-field) terrace surface and the planar top of the terrace gravel; 3.3 m and 3.8 m are the respective amounts of their vertical offset. *abcdef* and *gf* are segments of gravel surface exposed in the trench, where *ab* and *gf* are segments of the original gravel surface, *bc* and *de* are portions of a degraded fault scarp and *cd* and *ef* are steeper segments above two fault planes (see text for details). (B) Log of the southern wall of trench A (see Fig. 8 for location). For tephra codes see Fig. 9 and Table 1. The ages of tephra layers are in ^{14}C years BP. Photo is oblique view of gravelly colluvial wedge (see text). (C) Palaeoseismic interpretation. UC = unconformities; CW = colluvial wedge. Numbers in the labels for unconformities and colluvial wedges correspond to the number of the palaeoseismic event concerned. EF = East fault plane; WF = West fault plane. See text for discussion.

and *de*, dipping west at the angles of 20 to 40°, are parts of an older degraded gravel scarp, and that segments *cd* and *ef* mark the position of two faults cutting the gravels (faults EF and WF in Fig. 11C).

Above the original gravel surface (above segments *ab* and *gh*) the base of the cover sequence comprises a bright yellow loam about 20 cm thick that is overlain by the KZ tephra (KZ 7550 in Fig. 11B), extending parallel to the gravel surface. On the upthrown side of the fault the loam layer thins and disappears as it approaches the crest of the buried gravel scarp, so that the overlying KZ tephra here merges with the gravel. The absence of any loam-containing gravelly colluvial material at the scarp and the fact that the crest of the gravel scarp is west of where loam disappears indicate that the scarp predates loam accumulation. Accordingly, the succession of events is inferred as follows: 1) fault displacement of the gravel, 2) collapse and degradation of the fault scarp, 3) accumulation and coeval downslope movement of the loam, maintaining the upper portion of the scarp as a free face, 4) KZ tephra fall.

In view of this an estimate of the upper time limit for the faulting event is a combination of the KZ layer age (7550 ^{14}C years BP or about 8.3 to 8.4 ka of calibrated years) and about 2 ka, the time interval needed for accumulation of about 20 cm of loam. This gives around 10.5 ka years BP as the minimum age of the faulting event.

7.2. Event 2

Higher in the section, another apparent event horizon is represented by an angular unconformity within the fault-related graben. This occurs between the KZ/KL tephra layers and the overlying SH_{4800} tephra (Fig. 11B and C). On the footwall side, the event horizon is the erosional surface that truncates, with gentle westerly dip, the KL. There are only fragments of the SH_{4800} layer above this surface but the age of the event can be constrained as bracketed by the KL and SH_{4800} tephra layers. Judging by the extent of one minor reverse fault beyond the KL layer and estimating the accumulation rate for the sediments between the ashes at about 0.2 mm year^{-1}, some 500 years might be expected to have passed between the faulting event and the SH_{4800} tephra fall (about 5500 calibrated years BP). This suggests the event took place about 6 ka BP.

7.3. Event 3

A similar but younger unconformity exists between the SH_{4800} tephra layer and the Gamchen 3100 tephra (labelled GA in Fig. 11B). On the outer (western) side of the graben the SH_{4800} layer is offset by a minor reverse fault that extends several cm above this layer but does not deform the Gamchen tephra. The exact stratigraphic position of the unconformity cannot be defined precisely but is indicated by the offset amount on the SH_{4800} tephra layer, which is about 14 cm. This 14 cm represents a minimum thickness of material that accumulated on the SH_{4800} tephra before the faulting event. Consequently, the unconformity is expected to lie much closer to the Gamchen tephra. Subtracting the estimated duration, in years, for accumulation of a soil–pyroclastics layer exceeding 14 cm (~1000 years) from the calibrated age of the SH_{4800} tephra (5500 years), we obtain about 4500 years BP as the age of the event.

7.4. Event 4 and Event 5

The next two events apparently occurred in relatively quick succession and are each indicated by distinct colluvial wedges. The lower wedge (CW4 in Fig. 11C) includes Gamchen and KL tephra layers, both deformed into east-vergent folds. Its western part, recognized by the presence of fragments of both tephra layers, is in tectonic contact with the west fault plane (WF in Fig. 11C) and is overlain there unconformably by a thin layer of unnamed black ash that lies between the Gamchen and KZ-3000 tephra layers immediately above it (see Fig. 11B). Eastwards, CW4 extends so that it makes depositional contact with the gravel scarp above the EF fault plane (Fig. 11C).

The higher colluvial wedge can be subdivided into an entirely gravely lower part ($CW5_1$) and a generally finer, although with rare granules and pebbles, upper part ($CW5_2$). $CW5_1$ directly overlies the same unnamed thin black ash that covers the older CW4 wedge. These relationships suggest that the lower gravely part of CW5 formed when the gravels became exposed at the ground surface by vertical movement on WF, while the finer upper part of the colluvial material resulted from much slower post seismic downslope movement of cover material. The KZ-3000 tephra that lies within the finer upper part of the wedge ($CW5_2$) provides an upper time limit for CW5.

From the above, it follows that both wedges formed successively within a relatively short time span of some 200 years, between the Gamchen and KZ-3000 tephra falls. First, displacement took place on the east fault (EF in Fig. 11C) followed by downslope movement of the soil–pyroclastic material and formation of CW4. This faulting event (Event 4) occurred just before the black ash fall. Shortly after, movement

on the west fault (WF in Fig. 11C) displaced CW4 and caused formation of CW5 (Event 5). The fine upper portion of CW5 is composed partially of reworked material from CW4. In our tephra reference frame, the two events occurred one after another, about 3.2–3.3 thousand calibrated years ago.

In summary, we distinguish five faulting events, as enumerated above, occurring at about 10.5 ka, 6 ka, 4.5 ka and 3.2–3.3 ka BP. No faulting has occurred since the KZ-3000 tephra fall (ca. 3200 cal. years BP). Measured by vertical separation of CW4, the vertical displacement in the most recent faulting event was about 1 m, which also corresponds to the vertical offset of the youngest river terrace (Profile C in Fig. 8). Roughly the same vertical displacement, 0.8 to 1 m, occurred during the penultimate event, as suggested by the amount of vertical offset of the gravel scarp above the east fault plane (between segments *bc* and *de* in Fig. 11A). However, there are no clear and reliable indicators of how the remaining 1.8–2 m of net vertical slip (from a total of about 3.8 m) may be apportioned between the first three events. On average, each of them may have contributed around 0.6–0.7 m. Since fault planes exposed in the trench are nearly vertical, the above values of vertical separations provide reliable estimates of amounts of dip-slip component of fault movement.

Absence of fault movements younger then ~3000 years is also consistent with a minor trench C dug across the fault scarp on the younger river terrace (Fig. 12, see Fig. 8 for location). In that trench, the soil–pyroclastic sequence beginning with the KZ-3000 tephra just mantles the gravel scarp and is apparently unfaulted.

8. Discussion

8.1. Holocene faulting

Palaeoseismic studies such as ours aim to provide detailed information but as a consequence are inevitably limited in areal coverage. Moreover, the topographically most prominent faults within a fault zone are often problematic for palaeoseismic work because they are associated with high energy erosional and depositional settings unlikely to preserve the continuous and detailed records sought (Rust, 1993, 2005). This is underlined by the present study since, in order to exploit the detailed tephra chronology, stable surfaces are required, while at the same time being cut and displaced by faulting. The sites chosen proved ideal since the faulting generated scarps sufficient to produce distinct colluvial wedges, yet the highly permeable materials were not prone to surface runoff.

Our palaeoseismic data from the fault that crosses the Bol'shaya Khapitsa valley show that Holocene faulting in Central Kamchatka may occur in pulses, and that the recurrence interval may be rather long, reaching up to 3000 years or more. Methodologically, our work demonstrates that palaeoseismic techniques involving trench excavations can successfully be applied in volcanic terrains. This employs particularly the extensive use of crosscutting and stratigraphic relationships between fault-related structures and pyroclastic deposits, when the latter are well correlated on a regional basis.

The trench record indicates there have been five Holocene faulting events, with recurrence interval of up to 3000 years and a single-event dip-slip component of

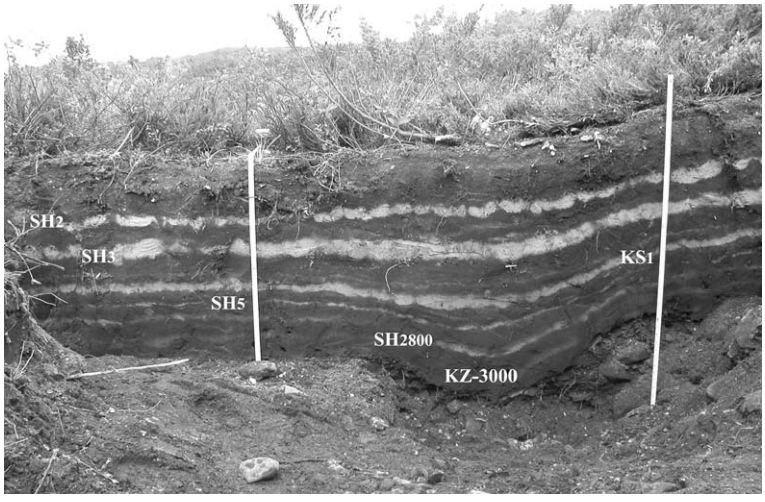

Fig. 12. Photo of the north wall of trench C (see Fig. 8 for location).

movement reaching about 1 m. Together with the inferred right-lateral component, the single-event total fault movement may amount to some 1.25 m. Judging by both this value and the characteristic length of individual surface faults of the EKFZ, faulting-related earthquakes may reach 6.5 and above in moment magnitude (Wells and Coppersmith, 1994). Moreover, since the most recent event occurred some 3000 years ago, future ground rupture may be imminent. Therefore, our work clearly indicates that it is necessary to evaluate the seismic potential of the EKFZ, especially near populated areas, in addition to that related to subduction of the Pacific plate beneath Kamchatka.

However, as shown by the mapping in Figs. 3 and 4, our trenches exposed a record for only one of the faults making up the EKFZ, thus raising the question of its applicability to the fault zone as a whole.

The fault studied within the Bol'shaya Khapitsa valley shows a smaller component of vertical movement compared to the Kumroch fault. The observed vertical offset of the highest river terrace gravel (3.8 m), and the time interval between the first (Event 1) and the most recent (Event 5) fault movements (about 6500 years) yields an average vertical displacement rate of about 0.6 mm $year^{-1}$, 3 to 4 times slower than that on the Kumroch fault (see Section 4). This corresponds well with the reduction in vertical displacement expressed topographically on the fault investigated (~200 m) compared to that on the Kumroch fault (~1000 m). This suggests along-strike variation in vertical movement on the EKFZ, as well as probable segmentation.

Our data on the geomorphic expression of the EKFZ fault in the Kumroch area show that post-glacial fault kinematics combines right-lateral and normal components. Farther south, similar findings from the central and southern parts of the CKD eastern boundary (Kozhurin, 1988) suggest that these kinematics may be taken as representative of the entire portion of the East Kamchatka Fault Zone that borders the depression. However, at a larger scale, as suggested above, along-strike variation and segmentation can be expected. The EKFZ stretches over two thirds of the Kamchatka Peninsula. In the north, it starts north of the CKD, in the Kamchatsky Peninsula, and in the south it seems to end at the Nachiki Transverse Zone (Fig. 2). Thus, together with the Nachiki Transverse Zone, the EKFZ appears to form the western margin of a block moving separately from the rest of Kamchatka. The Nachiki Transverse Zone may therefore be interpreted as accommodating right-lateral slip along the EKFZ Zone. Correspondingly, broad depressions within the Kamchatsky Peninsula, at the opposite end of the fault zone, may have developed due to strike-slip-related extension. In our interpretation, the EKFZ may be comparable to other major fault zones of the Pacific north and northwestern periphery, all of which exhibit some component of dextral strike-slip movement (Kozhurin, 2004).

The dip-slip component of displacement on the EKFZ is only pronounced where it forms the eastern margin of the Central Kamchatka Depression, providing additional evidence for the extensional nature of this basin. However, this tectonic regime may be difficult to reconcile with the idea of the western Aleutians actively colliding with Kamchatka (Geist and Scholl, 1994).

One plausible model that could account for extension on the CKD eastern margin may be slab roll-back with related east-directed movement of the eastern Central Kamchatka block including the East Kamchatka Ranges. In that case some transverse (approximately on strike with the western Aleutians) fault structures would be expected extending from the north of the CKD through the East Kamchatka Ranges to the trench, yet none have been found so far. Alternatively, the extension may also reflect the westward movement of Central Kamchatka, including CKD, away from the East Kamchatka Ranges. The possible mechanism for such block movement could be shear stress applied to the Kamchatka arc crust by deforming upper mantle, as suggested by Levin et al. (2002) based on observed anisotropy in the mantle wedge.

8.2. Relationships with main volcanic events

The data presented here on Holocene faulting events do not permit any comprehensive correlation to volcanic activity; however, it is tempting to compare at least some of the dated faulting events to the eruptive histories of adjacent volcanoes (Fig. 13).

The period around the two closely spaced faulting events that took place about 3.2–3.3 ka ago is notable for the abundance of mafic eruptive products, these being especially unusual for Kizimen, Shiveluch and Gamchen volcanoes. Eruptions from Gamchen and Shiveluch preceded the faulting events, while eruptions in the Kliuchevskoi group and at Kizimen immediately followed them. This cluster of mafic eruptions in the region, combined with the close timing of the two faulting events may indicate stress redistribution at depth. The timing of the eruptions may also reflect different storage levels of varying types of magma.

Unfortunately, the rarity of marker tephra layers of early Holocene age in the region does not allow precise dating of older faulting events, or of the eruptive periods

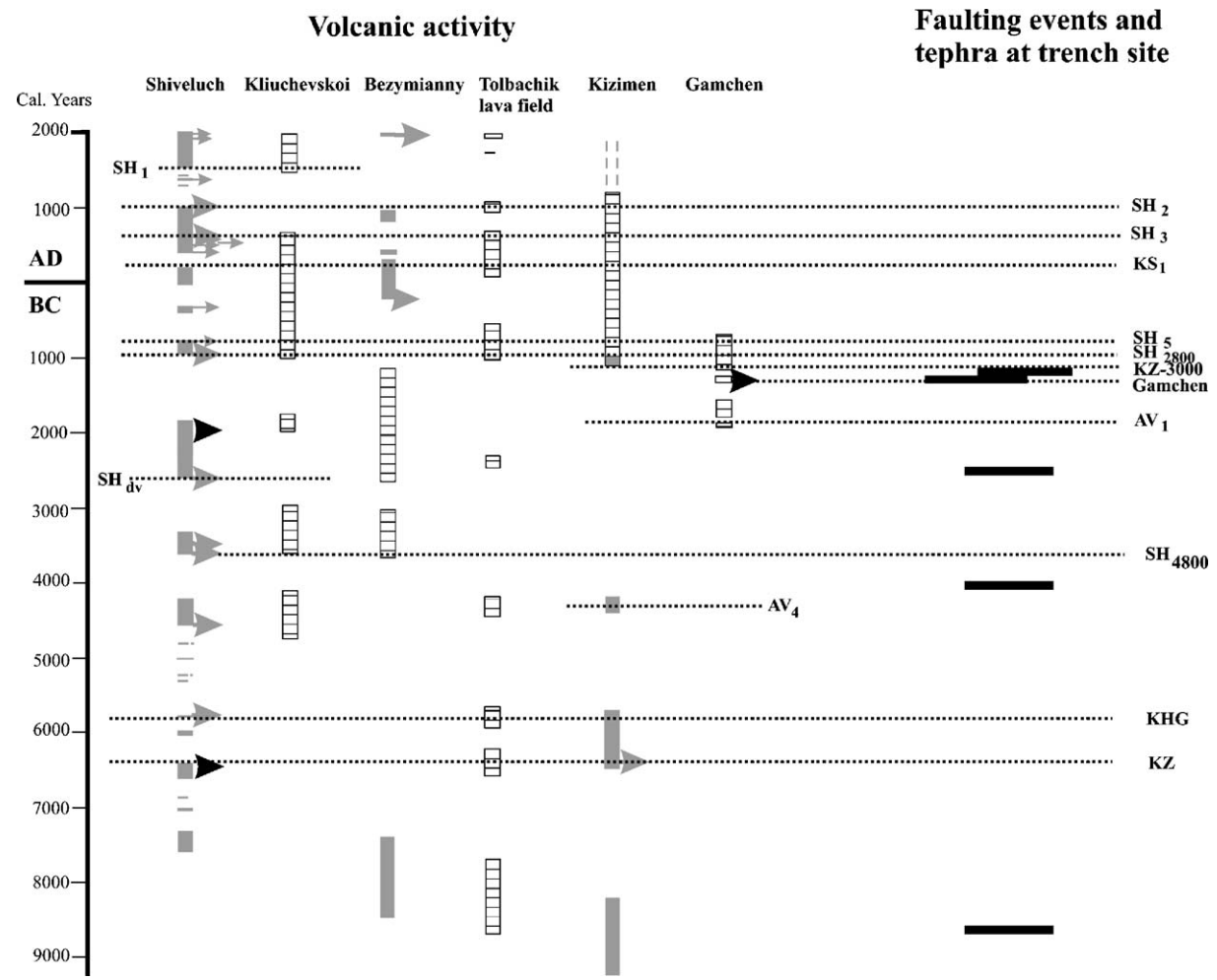

Fig. 13. Correlation between volcanic activity and faulting events. Vertical bars denote continuous volcanic activity (hatched for basalts and basaltic andesites, and grey for andesites and dacites), with arrows marking most prominent eruptions (black for basalts and basaltic andesites, and grey for andesites and dacites). Horizontal dotted lines are marker tephra layers (labeled as in Figs. 9 and 10 and Table 1). Faulting events are shown by solid black horizontal bars.

of that time at Tolbachik and Kliuchevskoi. However, we note that the faulting event about 6 ka BP is close in time to active periods at Shiveluch, Tolbachik and Kizimen (Braitseva et al., 1984; Melekestsev et al., 1995; Ponomareva et al., 1998), and the event about 4.5 ka BP to active periods at Shiveluch, Tolbachik and to the initiation of the Bezymianny volcano (Braitseva et al., 1991). It may also be significant that all the faulting events are accompanied by eruptions but the opposite does not occur (Fig. 13).

9. Conclusions

1). This multidisciplinary study focused on post-glacial alluvial terraces along the southern part of a segment of a major late Quaternary fault system affecting north-central Kamchatka. Trenching across the fault yielded evidence for five faulting events recorded in a Holocene succession containing numerous distinct and dated tephra layers. The oldest event occurred at about 10.5 ka BP followed by another at about 6 ka and another at about 4.5 ka BP. The final two events were closely spaced in time about 3.2–3.3 ka ago and since then no further events are recorded, despite a complete tephra succession extending up to recent historical eruptions. It may be that the fault zone is characterised by pulses of activity and that renewed faulting is imminent, with the capacity to generate significant regional shallow earthquakes (~M6.5). Such earthquakes constitute a source to be considered in seismic hazard

evaluations in addition to earthquakes related to the subduction of the Pacific Plate beneath Kamchatka.

2). Two major faults, including the Kumroch fault, dip NW and are characterized by combined normal and dextral motion. This suggests that the entire East Kamchatka Fault Zone (EKFZ) may move as an active dextral transtensive zone, with the normal component particularly significant on the segment of the zone that forms the eastern margin of the Central Kamchatka Depression. Moreover, displacement on this fault zone, together with slip on the Nachiki Transverse Zone farther south may define a regional-scale block moving ESE separately from the rest of Kamchatka.

3). There may be some correlation between faulting events and the activity of the nearest volcanoes. In fact, all the faulting events are accompanied by eruptions, but the opposite does not occur. This correlation may reflect changes in stress fields at depth that squeeze (mafic) magma to the surface and cause brittle deformation in the crust.

Acknowledgements

This research was supported by NATO–Russia Cooperative Linkage grant number JSTC.RCLG.978989 and grants to Vera Ponomareva and Ivan Melekestsev from the Russian Foundation for Basic Research. Field work was funded in part by grant 7664-04 from the National Geographic Society. This is a contribution to project UNESCO-IUGS-IGCP 455. We thank Dick Stewart for his help with mineralogical study of ash samples, and gratefully acknowledge the help of Mike Sandiford as Editor in Chief as well as helpful reviews from two anonymous reviewers.

References

Bazanova, L.I., Pevzner, M.M., 2001. Khangar: one more active volcano in Kamchatka. Transactions (Doklady) of the Russian Academy of Sciences. Earth Science Sections 377A, 307–310.

Bourgeois, J., Pinegina, T.K., Ponomareva, V.V., Zaretskaia, N.E., 2006. Holocene tsunamis in the southwestern Bering Sea, Russian Far East, and their tectonic implications. The Geol. Soc. Amer. Bull. 11 (3/4), 449–463. doi:10.1130/B25726.1.

Braitseva, O.A., Melekestsev, I.V., Evteeva, I.S., Lupikina, E.G., 1968. Stratigraphy of Quaternary Deposits and Glaciation of Kamchatka. Nauka, Moscow. 227 pp. (in Russian).

Braitseva, O.A., Melekestsev, I.V., Flerov, G.B., Ponomareva, V.V., Sulerzhitsky, L.D., Litasova, S.N., 1984. Holocene volcanism of the Tolbachik regional zone of cinder cones. In: Fedotov, S.A. (Ed.), Great Tolbachik Fissure Eruption, Kamchatka, 1975–1976. Nauka, Moscow, pp. 177–209 (in Russian).

Braitseva, O.A., Melekestsev, I.V., Bogoyavlenskaya, G.E., Maksimov, A.P., 1991. Bezymianny volcano: eruptive history and activity dynamics. Volcanol. Seismol. 12/2, 165–194.

Braitseva, O.A., Sulerzhitsky, L.D., Litasova, S.N., Melekestsev, I.V., Ponomareva, V.V., 1993. Radiocarbon dating and tephrochronology in Kamchatka. Radiocarbon 35/3, 463–476.

Braitseva, O.A., Melekestsev, I.V., Ponomareva, V.V., Sulerzhitsky, L. D., 1995. The ages of calderas, large explosive craters and active volcanoes in the Kuril–Kamchatka region, Russia. Bull. Volcanol. 57/6, 383–402.

Braitseva, O.A., Melekestsev, I.V., Ponomareva, V.V., Kirianov, V.Yu., 1996. The caldera-forming eruption of Ksudach volcano about cal. AD 240, the greatest explosive event of our era in Kamchatka. J. Volcanol. Geotherm. Res. 70/1–2, 49–66.

Braitseva, O.A., Sulerzhitsky, L.D., Ponomareva, V.V., Melekestsev, I. V., 1997a. Geochronology of the greatest Holocene explosive eruptions in Kamchatka and their imprint on the Greenland glacier shield. Transactions (Doklady) of the Russian Academy of Sciences. Earth Sci. Sect. 352/1, 138–140.

Braitseva, O.A., Ponomareva, V.V., Sulerzhitsky, L.D., Melekestsev, I. V., Bailey, J., 1997b. Holocene key-marker tephra layers in Kamchatka, Russia. Quat. Res. 47, 125–139.

Braitseva, O.A., Bazanova, L.I., Melekestsev, I.V., Sulerzhitsky, L.D., 1998. Largest Holocene eruptions of Avachinsky volcano, Kamchatka. Volcanol. Seismol. 20, 1–27.

Caskey, S.J., 1995. Geometric relations of dip slip to a faulted ground surface: new nomograms for estimating components of fault displacement. J. Struct. Geol. 17, 1197–1202.

Churikova, T., Dorendorf, F., Woerner, G., 2001. Sources and fluids in the mantle wedge below Kamchatka, Evidence from across-arc geochemical variation. J. Petrol. 42/8, 1567–1593.

DeMets, C.R., Gordon, R.G., Argus, D.F., Stein, S., 1990. Current plate motions. Geophys. J. Int. 101, 425–478.

Erlich, E.N., 1973. Modern Structure and Quaternary Volcanism of the Western Pacific Rim. Nauka, Novosibirsk. 243 pp. (in Russian).

Erlikh, E.N., Melekestsev, I.V., Shantser, A.E., 1974. Neotectonics. History of Relief Development in Siberia and Far East. Kamchatka, the Kuril and Komandor Islands. Nauka, Moscow, pp. 345–368 (in Russian).

Fedorov, P.I., Shapiro, M.N., 1998. Neogene volcanics of the Kamchatka isthmus and geodynamics of the Aleutian–Kamchatka junction. Geotectonics 32, 122–137.

Fedotov, S.A., Masurenkov, Yu.P. (Eds.) 1991. Active volcanoes of Kamchatka. Nauka, Moscow, Vol. 1: 302 pp. Vol. 2: 415 pp. (in Russian).

Florensky, I.V., Trifonov, V.G., 1985. Neotectonics and volcanism in the East Kamchatka volcanic zone. Geotektonika 4, 78–87 (in Russian).

Gaedicke, C., Baranov, B., Seliverstov, N., Alexeiev, D., Tsukanov, N., Freitag, R., 2000. Structure of an active arc–continent collision area: the Aleutian–Kamchatka junction. Tectonophysics 325, 63–85.

Geist, E.L., Scholl, D.W., 1994. Large-scale deformation related to the collision of the Aleutian Arc with Kamchatka. Tectonics 13 (3), 538–560.

Gorbatov, A., Kostoglodov, V., Suarez, G., Gordeev, E.I., 1997. Seismicity and structure of the Kamchatka subduction zone. J. Geophys. Res. B 102 (8), 17883–17898.

Gordeev, E.I., Gusev, A.A., Levina, V.I., Leonov, V.L., Chebrov, V.A., 2004. Crustal seismicity of Kamchatka. AGU Fall Meeting. EOS Trans. AGU, 85(47), Fall Meet. Suppl., Abstract T11D-1282.

Hochstaedter, A.G., Kepezhinskas, P.K., Defant, M.J., Drummond, M. S., Bellon, H., 1994. On the tectonic significance of arc volcanism in northern Kamchatka. J. Geol. 102, 639–654.

Kepezhinskas, P.K., 1987. Origin of Cenozoic volcanic series of Komandorsky basin framing according to geochemical and experimental data. Geologicky Zbornik-Geologica Carpathica 38, 71–81.

Konstantinovskaya, E.A., 2003. Margins of East Asia: tectonics, structural evolution and geodynamic modeling. Transactions 549 Scientific World, Moscow, 223 pp. (in Russian).

Kozhurin, A.I., 1988. The Kuril–Kamchatka island arc: neotectonic zoning, Late Quaternary structure of Central Kamchatka, tectonic layering of the lithosphere in Central Kamchatka, some general features of the neotectonic structures of the circum-Pacific mobile belt. In: Neotektonika i sovremennaya geofinamika podvizhnykh poyasov. Nauka, Moskva, pp. 67–115 and 135–151 (in Russian).

Kozhurin, A.I., 1990. Recent strike-slip faults in the Kumroch Range and Kamchatsky peninsula area, Eastern Kamchatka. Tikhookeanskaya Geologiya 6, 45–55 (in Russian).

Kozhurin, A.I., 2004. Active faulting at the Eurasian, North American and Pacific plates junction. Tectonophysics 380, 273–285.

Lander, A.V., Bukchin, B.G., Droznin, D.V., Kiryushin, A.V., 1994. The tectonic environment and source parameters of the Khailino, Koryakiya earthquake of March 8, 1991: Does a Beringia plate exist? Comput. Seismol. 3, 80–96 (English edition of the Geodinamika i prognoz zemletriaseniy. Vychislitel'naya seismologiya).

Legler, V.A., 1976. Deformation of the subducting lithospheric plate and longitudinal shifts of the Kuril–Kamchatka island arc. Tectonics of the Lithospheric Plates (Dynamics of the Subduction Zone). P.P.Shirshov. Institute of Oceanology AN SSSR, Moscow, pp. 103–147 (in Russian).

Levin, V., Shapiro, M., Park, J., Ritzwoller, M., 2002. Seismic evidence for catastrophic slab loss beneath Kamchatka. Nature 418, 763–767.

Mackey, K., Fujita, K., Gunbina, L., Kovalev, V., Imaev, V., Koz'min, B., Imaeva, L., 1997. Seismicity of the Bering Strait region: evidence for a Bering block. Geology 25/11, 979–982.

Melekestsev, I.V., 1974. Main stages of development of the modern relief of the Kuril–Kamchatka region. In: Luchitsky, I.V. (Ed.), History of Relief Development in Siberia and Far East. Kamchatka, the Kuril and Komandor Islands. Nauka, Moscow, pp. 337–344 (in Russian).

Melekestsev, I.V., 1980. Volcanism and Relief Formation. Nauka, Moscow. 212 pp. (in Russian).

Melekestsev, I.V., Ponomareva, V.V., Volynets, O.N., 1995. Kizimen volcano (Kamchatka)—future Mt. St. Helens? J. Volcanol. Geotherm. Res. 65, 205–226.

Park, J., Levin, V., Lees, J., Peyton, V., Gordeev, E., Ozerov, A., 2002. A dangling slab, amplified arc volcanism, mantle flow and seismic anisotropy in the Kamchatka Plate Corner. In: Stein, S., Freymueller, J.T. (Eds.), Plate Boundary Zones. Geodynamics Series, vol. 30, pp. 295–324.

Pevzner, M.M., Ponomareva, V.V., Melekestsev, I.V., 1998. Chernyi Yar—reference section of the Holocene ash markers at the northeastern coast of Kamchatka. Volcanol. Seismol. 19/4, 389–406.

Ponomareva, V.V, Pevzner, M.M, Melekestsev, I.V., 1998. Large debris avalanches and associated eruptions in the Holocene eruptive history of Shiveluch volcano, Kamchatka, Russia. Bull. Volcanol. 59/7, 490–505.

Ponomareva, V.V, Pevzner, M.M, Sulerzhitsky, L.D., 2002. Explosive activity of Shiveluch volcano, Kamchatka, during the last 10,000 years. Abstracts of the 3rd Biennial Workshop on Subduction processes. Fairbanks, Alaska, June 2002.

Rust, D.J., 1993. Recognition and assessment of faults within active strike-slip fault zones: a case study from the San Andreas fault in southern California. In: Stewart, I., Vita-Finzi, C., Owen, L. (Eds.), Neotectonics and Active Faulting. Zeits fur Geomorph, vol. 94, pp. 207–222. Suppl.-Bd.

Rust, D., 2005. Palaeoseismology in steep terrain: the Big Bend of the San Andreas fault, Transverse Ranges, California. Tectonophysics 408, 193–205 Special Volume on Palaeoseismology.

Stuiver, M., Reimer, P.J., Bard, E., Beck, J.W., Burr, G.S., Hughen, K. A., Kromer, B., McCormac, G., van der Plicht, J., Spurk, M., 1998. INTCAL98 Radiocarbon Age Calibration, 24,000–0 cal BP. Radiocarbon 40 (3), 1041–1085.

Svyatlovsky, A.E., 1967. Outline of History of Quaternary Volcanism of Kamchatka. Nauka, Moscow. 219 pp. (in Russian).

Tikhonov, V.I., 1968. Thrusts faults in East Kamchatka. Geotektonika 3, 88–101 (in Russian).

Volynets, O.N., Ponomareva, V.V., Braitseva, O.A., Melekestsev, I.V., Chen, Ch.H., 1999. Holocene eruptive history of Ksudach volcanic massif, South Kamchatka: evolution of a large magmatic chamber. J. Volcanol. Geotherm. Res. 91, 23–42.

Wells, D.L., Coppersmith, K.J., 1994. New empirical relationships among magnitude, rupture length, rupture width, rupture area, and surface displacement. Bull. Seismol. Soc. Am. 84, 974–1002.

Yogodzinski, G.M., Lees, J.M., Churikova, T.G., Dorendorf, F., Wörner, G., Volynets, O.N., 2001. Geochemical evidence for the melting of subducting oceanic lithosphere at plate edges. Nature 409, 500–504.

Zonenshain, L.P., Savostin, L.A., 1979. Introduction to Geodynamics. Nedra, Moscow. 311 pp. (in Russian).